IEEE Access
Multidisciplinary | Rapid Review | Open Access Journal

Received February 19, 2021, accepted March 1, 2021, date of publication March 4, 2021, date of current version March 12, 2021.

Digital Object Identifier 10.1109/ACCESS.2021.3063885

An Ensemble Approach Based on Multi-Source Information to Predict Drug-MiRNA Associations via Convolutional Neural Networks

K. DEEPTHI[1,2], (Member, IEEE), AND A. S. JEREESH[1]

[1]Bioinformatics Lab, Department of Computer Science, Cochin University of Science and Technology, Kochi 682022, India
[2]Department of Computer Science, College of Engineering Vadakara (CAPE, Government of Kerala), Kozhikode 673104, India

Corresponding author: K. Deepthi (deepthi523@gmail.com)

ABSTRACT Increasing evidence from recent research demonstrates that aberrant expressions of microRNAs (miRNAs) are linked to the development of chronic human diseases. Targeting miRNAs with bioactive small-molecules (or drugs) to regulate their activities provide an innovative insight into human disease treatment. Identifying the drugs that target particular miRNAs through the experimental study is complicated, time-consuming, and tremendously expensive. Therefore, computational researches by integrating information on drugs and miRNAs are essential for discovering potential drug-miRNA associations. Realizing the appropriate drugs that target the causal miRNAs behind diseases will contribute to miRNA mediated disease therapeutics and drug clinical applications. This study proposes an ensemble learning approach, ELDMA, that predicts novel drug-miRNA associations based on deep architecture-based classification. The method constructed features based on the integrated pairwise similarities of drugs and miRNAs and reduced the feature dimensions with principal component analysis (PCA). With the resulting features, the convolutional neural network is trained to extract intricate, high-level patterns. The deep retrieved features are given to the support vector machine classifier to infer potential drug-miRNA associations. We conducted global leave-one-out cross-validation (LOOCV), drug-fixed local LOOCV, miRNA-fixed local LOOCV, and 5-fold cross-validation to evaluate the model performance. ELMDA achieved corresponding AUCs of 0.9862, 0.7426, 0.9847 and 0.9928 for Dataset 1 and AUCs of 0.8643, 0.6742, 0.8671 and 0.8521 for Dataset 2, respectively. The results and case studies illustrate the effectiveness of ELDMA in identifying novel drug-miRNA candidates. The top predicted relationships are released for future wet-lab studies.

INDEX TERMS Convolutional neural network, disease, drug, MiRNA, PCA, support vector machine.

I. INTRODUCTION

MiRNAs are a novel class of non-coding RNAs involved in the process of RNA silencing and post-transcriptional regulation of gene expression [1], [2]. They are involved in many basic functions for the growth and development of living organisms. MiRNAs act as regulators of various cellular pathways [3], and they achieve their function by binding with the complementary sequences of mRNA molecules. Although the first MiRNA was found in the early 1990s in Caenorhabditis elegans [4], miRNAs gained increasing attention from researchers recently. Many recent experiments disclose that miRNAs play essential roles as biomarkers and treatment targets for chronic diseases [5], [6]. Abnormal miRNA expressions are correlated with complex diseases, including cancer, Parkinson's, and immune-related diseases [7], [8].

Most of the drugs are small molecules that bind with specific target molecules to achieve their therapeutic functions. Restoration of dysregulated miRNA expressions by small molecule drugs provides a novel and promising way for disease treatment. The particular secondary structure and conserved sequences make miRNAs suitable to be drug targets [9]. Drugs can act on different targets rather than a single target [10]. Therefore, drugs designed for a particular miRNA target can be used to target another miRNA. As drug discovery is high-cost and complicated, drug developers are struggling to discover alternate applications for known drugs. Since experimental methods for finding the relationships

The associate editor coordinating the review of this manuscript and approving it for publication was Chao Tong.

between drugs and miRNAs are expensive, computational approaches are vital for identifying novel drug-miRNA relationships [11].

As disclosed by the HMDD V3.0-Human miRNA Disease Database [12], there are about 35000 known miRNA-disease associations. Recently, many studies have been taken place to discover potential miRNA/non-coding RNA-disease associations [13]–[18]. However, very few researches have been conducted to analyze the drugs that can act on miRNAs systematically. Li *et al.* [19] suggested a network-oriented approach to identify novel drug-miRNA associations. They built a heterogeneous network consisting of drugs and MiRNAs. A method based on the topology information of the constructed network was used to infer potential drug-miRNA relationships. In brief, the algorithm situated the initial resources of the drug of interest to its adjacent miRNAs. The miRNAs partitioned these resources equally to their related drugs. The drugs in the last step allocated the obtained resources to their related miRNAs. Finally, the end resource score of each miRNA indicated its probability of being associated with the initial drug. Lv *et al.* [20] proposed a computational approach for predicting new drug-miRNA associations. They built a network that relied on the drug, miRNA pairwise similarities, and known associations between them. Next, they performed an improved version of the conventional random walk with restart algorithm by introducing the transition probability matrix, which enabled the random walker to walk on both the drug and miRNA networks rather than on the single-layer drug or miRNA network. Thus, the method could identify new miRNA targets for drugs without relying on whether the drug has any verified miRNA relationship.

Qu *et al.* [21] suggested a triple layer heterogeneous network-oriented approach for inferring new miRNAs associated with drugs. They utilized integrated drug, miRNA, disease similarities, and existing drug-miRNA and miRNA-disease relationships for network construction. Considering this network, they built two formulas that update iteratively to identify new drug-miRNA and miRNA-disease associations. The formulas were updated until the convergence criteria were met, and the final scores of the drug-miRNA association matrix were used to recognize novel miRNAs associated with drugs. Wang *et al.* [22] suggested a machine-learning approach to prioritize potential drug-miRNA relations. They constructed features based on drug and miRNA pairwise similarities and trained the random forest classifier with these features to identify new drug-miRNA associations. Qu *et al.* [23] introduced a network-based method for predicting novel miRNAs associated with drugs. They built a heterogeneous network utilizing the drug, miRNA similarities, and the confirmed associations among them. The method then calculated the relevance score between the drugs and miRNAs based on a path-based approach of HeteSim [24] in the constructed network. The HeteSim method calculates the affinity score between two nodes of the same or different types in the heterogeneous network considering the path that links the node pair through a sequence of nodes.

Guan *et al.* [25] developed a Graphlet Interaction based method for prioritizing novel miRNAs associated with drugs. They built a heterogeneous network by integrating information on the drug, miRNA similarities, and confirmed drug-miRNA associations. They assessed the affinity scores between drugs and miRNAs based on the number of graphlet interactions relied on the drug and miRNA similarity networks. Graphlet interaction describes the relation between any node pair in a graphlet, which is a kind of non-isomorphic subgraph in a large network. Deepthi and Jereesh [26] proposed a method predicting new drug-miRNA associations based on the inductive matrix completion (IMC) algorithm. The method aimed at identifying the unknown entries of the drug-miRNA association matrix, whose values indicate the probability of association for each drug-miRNA pair. They utilized drug and miRNA similarities as side information for the IMC algorithm. Liu *et al.* [27] proposed an approach for identifying new drug-miRNA relationships by utilizing multiple biological data and negative sample selection. They presented a method that selects highly credible negative drug-miRNA relationships, utilizing the similarity data. Next, they constructed a triple layer network that relied on drug, miRNA, and disease similarities and experimentally confirmed relationships between them. The method then performed the random walk with restart algorithm for new drug-miRNA relationship prediction. Negative sample selection improved the model performance by providing more reliable negative samples for validation instead of randomly choosing negative samples from unknown drug-miRNA relations.

Zhao *et al.* [28] conducted a study that utilized symmetric non-negative matrix factorization and regularized least squares to identify novel drug-miRNA relationships. They applied matrix factorization on the combined similarity matrices and computed the Kronecker product of the new matrices to derive similarities of drug-miRNA pairs. Then they applied regularized least square to identify new drug-miRNA relationships. Wang and Chen [29] proposed an approach considering the cross-layer dependency inference on heterogeneous networks to prioritize novel drug-miRNA candidates. In addition to drug-miRNA associations and drug, miRNA similarity data, they utilized miRNA-disease associations and disease similarity data for network construction. Considering the network topology and existing cross-layer relationships, they framed the drug-miRNA relationship prediction task as a regularized optimization problem. They solved the optimization problem using the block coordinate descent algorithm and built a feature matrix corresponding to each layer. Based on these matrices, they computed the drug-miRNA association score matrix to identify novel associations. Shen *et al.* [30] presented a computational method that relied on graph regularization techniques for inferring new miRNAs related to drugs. The method first built a heterogeneous network by incorporating drug-miRNA and miRNA-disease association data and their similarity information. Then the K-nearest neighbor profile method is applied to overcome the problems

of sparsity in the association data and handle the prediction of isolated items. Next, they fused multi-source information based on graph regularization techniques and computed the correlation score for each drug-miRNA pair by an iterative graph inference method.

Yin *et al.* [31] suggested a method based on sparse learning and heterogeneous graph inference for inferring new drug-miRNA relationships. First, they factorized the drug-miRNA association matrix using the sparse learning method (SLM) to eliminate noise present in the original data. Then, they constructed a heterogeneous network based on drug, miRNA similarity data, and the relationship data present in the association matrix after factorization. Finally, they computed the drug-miRNA correlation score by analyzing the path between the specific drug and miRNA in the constructed network. Luo *et al.* [32] conducted a study that predicts new drug-miRNA relationships relied on non-negative matrix factorization. They utilized drug, miRNA similarities, and existing associations between drugs and miRNAs to infer novel associations. They exploited the clinical and chemical information of drugs and miRNA-gene associations for similarity score calculation. To avoid overfitting and improve the model's predictive power, they incorporated a new objective function that relied on both graph Laplacian and Tikhonov regularizations into the non-negative matrix factorization to discover new drug-miRNA relationships.

Here, we present an ensemble method, ELDMA, that predicts novel drug-miRNA associations. ELDMA involves three main steps: PCA-based dimension reduction, convolutional neural network-based feature extraction, and support vector machine (SVM)-based classification. Ensemble approaches combine results from multiple learning algorithms to produce more accurate results. Far as we know, the neural network-relied approach is applying the first time for drug-miRNA relationship prediction. ELDMA combines multiple sources of information, including drug similarities based on chemical structure, functional consistency, side effect, and miRNA similarities considering their target genes and target diseases. The method constructed features based on these similarities and minimized the feature dimension with the PCA. With the reduced dimensional features, the convolutional neural network is trained to retrieve the implicit input patterns. The extracted features are sent to the SVM classifier to infer new drug-miRNA relations. The predicted candidates with probabilities above the threshold are regarded as novel drug-miRNA associations, and they are promising candidates for future biological tests. ELMDA obtained AUCs of 0.9862, 0.7426, 0.9847 and 0.9928 for Dataset 1 and AUCs of 0.8643, 0.6742, 0.8671 and 0.8521 for Dataset 2, under global LOOCV, drug-fixed local LOOCV, miRNA-fixed local LOOCV and 5-fold cross-validation, respectively. We compared ELDMA performance with previous methods and other machine learning classifiers. We implemented the model with distinct datasets. The results and case studies reveal that ELDMA is a powerful and efficacious tool for identifying new drugs that target particular miRNAs.

II. MATERIALS AND METHODS

A. DATASETS

1) DRUG-miRNA ASSOCIATIONS

The experimentally verified drug-miRNA associations were downloaded from SM2miR v1.0 [33]. We acquired 664 experimentally verified drug-miRNA relationships from this database. We collected 831 drugs from SM2miR, DrugBank [34], and PubChem [35], and 541 miRNAs from SM2miR, HMDD [36], PhenomiR [37], and miR2Disease [38]. We constructed a dataset based on the 664 known drug-miRNA associations from SM2miR, the collected 831 drugs, and 541 miRNAs, termed it as Dataset 1. We constructed another dataset named Dataset 2 by retaining only drugs and miRNAs with at least one known association. Dataset 2 contains 664 associations between 39 drugs and 286 miRNAs. Corresponding to each dataset, an $N_d \times N_m$ association matrix A was defined based on equation (1).

$$\begin{cases} A\left(d\left(i\right), m\left(j\right)\right) = 1 & \textit{drug } d\left(i\right) \textit{ has an association with miRNA } m\left(j\right) \\ A\left(d\left(i\right), m\left(j\right)\right) = 0 & \textit{drug } d\left(i\right) \textit{ has no association with miRNA } m\left(j\right) \end{cases} \tag{1}$$

where N_d, N_m denote the total number of drugs and miRNAs in the dataset, respectively.

2) DRUG CHEMICAL STRUCTURE SIMILARITY

Drug chemical structures were obtained from the DRUG and COMPOUND sections of the KEGG LIGAND database [39], and their structural similarity S_c was computed by using SIMCOMP (http://www.genome.jp/tools/simcomp/). SIMCOMP is a graph-based method developed for measuring the structural similarity between two chemical compounds.

3) DRUG SIDE EFFECT SIMILARITY

The drug side effect-based similarity was calculated based on the presumption that drugs that share common side effects tend to be similar. The side effect similarity S_s between two drugs, i and j, was calculated based on the Jaccard score [40], according to equation (2).

$$S_s = Jaccard\ score = \frac{|M\left(i\right) \cap M(j)|}{|M\left(i\right) \cup M(j)|} \tag{2}$$

where $M\left(i\right)$ and $M\left(j\right)$ are the side effects obtained from the SIDER database [41] related to drug i and drug j. Here, $|X|$ denotes the cardinality of X.

4) GENE FUNCTIONAL CONSISTENCY-BASED SIMILARITY FOR MiRNAs AND DRUGS

The functional similarity of miRNAs based on their target genes S_{m_g} was computed relied on the presumption that if the target gene sets of two miRNAs have functional consistency,

the miRNAs will be similar. The target genes associated with each miRNA were downloaded from the webserver TargetScan [42]. Gene set functional consistency was computed using the Gene Set Functional Similarity (GSFS) method [43] to measure miRNA functional similarity based on their target genes. Using the same method, the drug functional similarity S_{f_g} was computed based on their target genes. The target genes related to the drugs were acquired from DrugBank [34] and Therapeutic Targets Database (TTD) [44].

5) DISEASE PHENOTYPE-BASED SIMILARITY FOR MiRNAs AND DRUGS

MiRNA (drug) similarities based on the target diseases were measured by considering the presumption that miRNAs (drugs) that share common diseases tend to be more similar. MiRNA-associated diseases were obtained from HMDD [36], miR2Disease [38], and PhenomiR [37]. The miRNA target disease-based similarity S_{m_d} was calculated using the Jaccard score according to equation (2). Here, $M(i)$ and $M(j)$ denote the disease sets associated with miRNA i and miRNA j, respectively. Similarly, the drug similarity S_{f_d} was computed based on the Jaccard score to specify the target disease-based similarity among drug i and drug j. The diseases associated with drugs were obtained from the Comparative Toxicogenomics Database (CTD) [45], DrugBank, and TTD.

6) DRUG-DRUG SIMILARITIES

The integrated drug pairwise similarity used in our study was calculated based on drug side effect similarity S_s [40], chemical structure similarity S_c [46], functional consistency based on their target genes S_{f_g} [43], and target diseases S_{f_d} [40]. The integrated drug similarity S_D was measured based on equation (3).

$$S_D = (\Upsilon_1 S_c + \Upsilon_2 S_{f_g} + \Upsilon_3 S_{f_d} + \Upsilon_4 S_s)/\sum_i \Upsilon_i \quad (\mathrm{i} = 1, 2, 3, 4) \tag{3}$$

Here, the default value $\Upsilon_i = 1$ denotes that each similarity is assigned the same weight.

7) MiRNA-miRNA SIMILARITIES

The integrated miRNA similarity S_M was measured by averaging the gene functional consistency-based and disease phenotype-based miRNA similarities [43], [40], according to equation (4).

$$S_M = (\mu_1 S_{m_g} + \mu_2 S_{m_d})/\sum_i \mu_i \quad (\mathrm{i} = 1, 2) \tag{4}$$

Here, the default value $\mu_i = 1$ indicates that each similarity possesses the same weight. We acquired the integrated drug and miRNA pairwise similarities from [20].

B. METHOD

In this work, we proposed an architecture for identifying novel drug-miRNA relationships that consist of 3 main segments: PCA, Convolutional neural network (CNN), and support vector machines (SVM). For each drug-miRNA pair (d_i, m_i) in the dataset, we built feature vectors considering the integrated similarities of drugs and miRNAs. Feature vector $FV(d_i)$ for the drug d_i includes integrated similarities of d_i to all other drugs in the dataset, equation (5). Similarly, the feature vector $FV(m_i)$ for the miRNA m_i includes integrated similarities of m_i to all other miRNAs in the dataset equation (6).

$$FV(d_i) = [f_1, f_2, f_3, \ldots\ldots, f_x \ldots\ldots, f_{N_d}] \tag{5}$$

$$FV(m_i) = [g_1, g_2, g_3, \ldots\ldots, g_x \ldots\ldots, g_{N_m}] \tag{6}$$

where f_i, g_i represent corresponding integrated similarities of drug d_i and miRNA m_i and N_d, N_m represent the total number of drugs and miRNAs, respectively, in the dataset. Since these feature vectors are very long and upon concatenation, they produce vectors with almost double size; we employed PCA for dimensionality reduction. The new drug, miRNA feature vectors with reduced sizes nd, nm, respectively, obtained from PCA output, were concatenated to build features with size $nd + nm$. We set nd and nm to 100 and 202, respectively, as these values gave optimum results. There were $N_d \times N_m$ such sample features; each corresponds to a drug-miRNA pair. The corresponding label was selected from the association matrix. The label was set to one if there is an existing relationship between the corresponding drug and the miRNA; otherwise, it was set to zero. The positive set comprises the samples with label one. We randomly picked unknown drug-miRNA relationships and created the negative set with the same size as the positive set. There is a possibility for unknown positive relationships in the created negative set, but the probability, $664 \div (831 \times 541 - 664) \approx 0.15\%$, can be neglected compared to the entire unverified relationships in the dataset. Finally, we constructed the training set with 1328 samples by combining the positive and negative sets. These features were sent to CNN to retrieve unique input patterns. With the retrieved deep features, the SVM classifier was trained to predict new drug-miRNA relationships and corresponding probabilities.

1) FEATURE EXTRACTION BASED ON CONVOLUTIONAL NEURAL NETWORK

CNN is a feed-forward neural network structure composed of three kinds of layers: convolution layer, subsampling layer, and fully connected layer. The power of a CNN lies in the particular layer called the convolutional layer. CNN contains multiple convolutional layers, and each one is capable of retrieving more sophisticated input patterns. CNN was proposed by LeCun *et al.* [47], and they were proved to be effective for the feature extraction and classification in prediction problems such as the identification of drug/circular RNA/long non-coding RNA-disease relationships [48]–[50]. This neural network structure consists of two main segments: feature extraction and classification. Feature extraction comprises multiple convolution and pooling layers followed by activation functions. The classifier is composed of fully

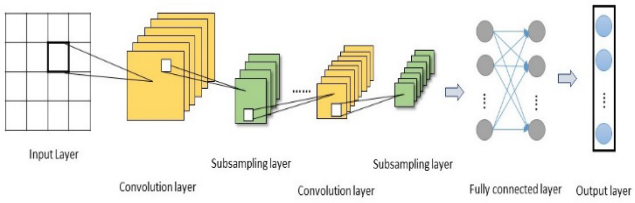

FIGURE 1. The basic architecture of CNN.

connected layers. In our study, we used CNN to extract high-level patterns from the input features. Convolutional and pooling layers can retrieve the special features from the input. We implemented the convolution operation on the concatenated input feature matrix with multiple convolution kernels to obtain the feature map. The parameters of the filters need to be learned. The convolution operation at layer t can be represented as:

$$X_t = £(X_{t-1} \otimes W_t + b_t) \tag{7}$$

W_t represents the convolution kernel weight matrix, b_t the offset vector, and X_t the feature map of layer t. $\otimes$ indicate the convolution operation and $£(k)$ the activation function. In the subsampling (pooling) layer, the sampling formula can be represented as:

$$X_t = Subsampling(X_{t-1}) \tag{8}$$

We used max-pooling to down-sample the latent features after the convolutional layer. It picks the maximum element from the region of the feature map covered by the filter. The convolutional layer and max-pooling layer can extract the best features from the input. The CNN is designed using alternate sets of convolution and subsampling layers, followed by the hidden layers. The training goal of CNN is to minimize the loss function of the network. The feature matrix corresponding to the training set was given to CNN to generate a matrix with essential features. We optimized the parameters of CNN by conducting a series of experiments. We selected the kernel size at convolution and pooling layers as 16×16 and 2×2, respectively. We used the sigmoid as the activation function, binary cross-entropy as the error function, and Adam as the optimization algorithm in model construction. Finally, the high-level features obtained after multiple convolution and pooling operations are extracted for association prediction. The basic structure of the CNN is depicted in Figure 1.

2) SUPPORT VECTOR MACHINE-BASED CLASSIFICATION

SVM is a powerful classification algorithm proposed by Vapnik *et al.* [51], [52] that partitions data into separate categories. SVM aims to construct a hyperplane that maximizes the margin between the two classes. They solve classification tasks by mapping training samples to points in space, such as it maximizes the distance between the two categories. The trained model maps new samples to that same space and predicts the class according to the side of the hyperplane they fall.

SVM has been previously applied to various biological problems, including identification of long non-coding RNA/microRNA-disease relationships [53]–[55], drug-target interaction predictions [56], identification of druggable proteins [57], etc. In the proposed method, the SVM classifier was trained with the compact high-level features obtained from the CNN after convolution and pooling operations. The trained classifier was able to predict novel drug-miRNA associations and their corresponding probabilities as the classification result. The drug-miRNA relationships with probabilities higher than the threshold were regarded as promising candidates for biological experiments. The complete workflow of the proposed model is outlined in Figure 2.

Based on our tests and prior studies [58], [59], we utilized Radial Basis Function (RBF) as the kernel in SVM. We implemented ELDMA with different combinations of similarity data, as Lv *et al.* [20], to analyze the impact of multiple similarity data on model performance. We obtained optimum results by combining the four drug similarity metrics and two miRNA similarity metrics, as described by equations (3) and (4).

III. RESULTS

A. PERFORMANCE EVALUATION

We adopted global and local LOOCV as well as 5-fold cross-validation to evaluate the model performance. In global LOOCV, each positive sample in the training set was considered as the test sample in turn, while the other positive samples were used for training. The test sample score is compared with the scores of all unknown samples in the dataset. Local LOOCV is conducted in two ways by fixing the drugs and by fixing the miRNAs. In the drug-fixed local LOOCV, the test sample score is compared with the scores of the candidate samples, which includes all unknown miRNA associations with the test drug. In the miRNA-fixed local LOOCV, the test sample score is compared with the scores of the candidate samples, which include all unknown drug associations with the test miRNA. In 5-fold cross-validation, the training set is segmented into 5 subsets with roughly equal size. When the method is executed, one subset was reserved for validation, and other subsets were used for training the model. The process was repeated 5 times until all subsets been validated once, and the average results were adopted for evaluation. In the cross-validation results, verified associations with predicted probabilities above the threshold were considered as True Positives (TP), and below the threshold were considered as False Negatives (FN). Similarly, unverified associations with predicted probabilities below the threshold were considered as True Negatives (TN), and above the threshold were considered as False Positives (FP).

We conducted cross-validation experiments using Dataset 1 and Dataset 2 and measured the true positive rate and false-positive rate by varying the thresholds. Based on this, the Receiver Operating Characteristic curves (ROC) [60], [61] are constructed and measured the Area Under the ROC curves (AUC) [62]. ELDMA obtained AUCs

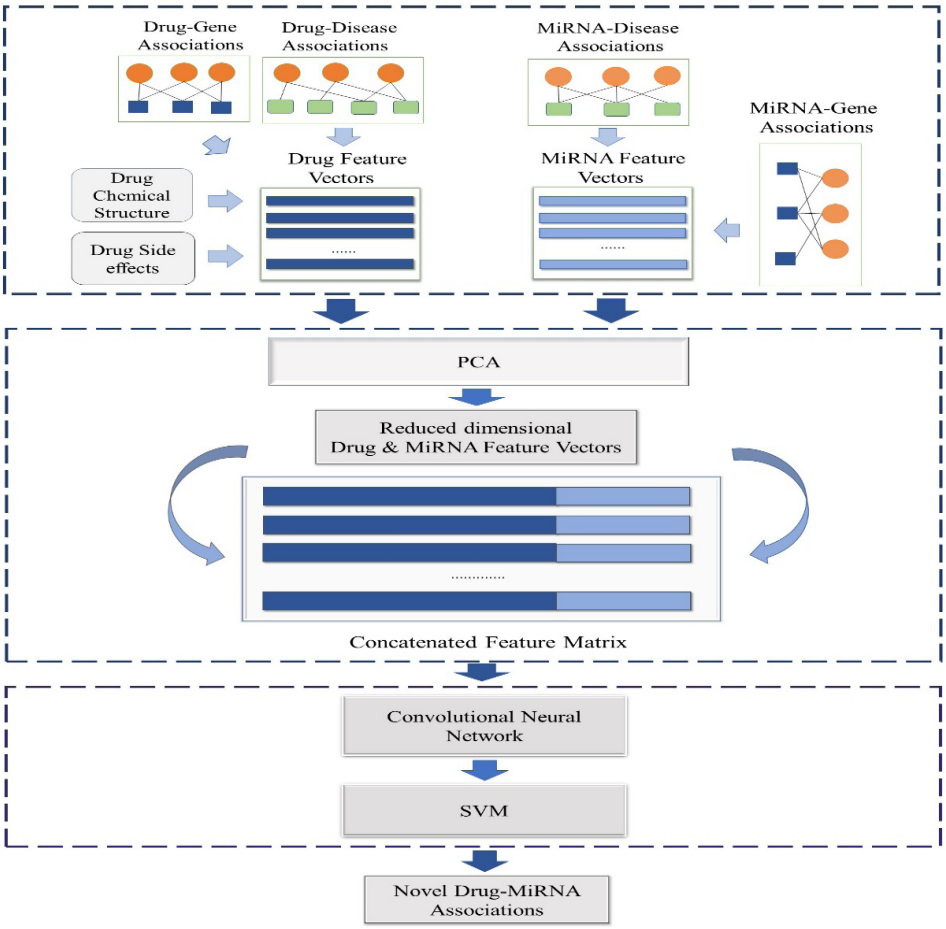

FIGURE 2. The flowchart of ELDMA to infer novel drug-miRNA relationships. With the integrated features of drugs and miRNAs as input, ELDMA consists of three main steps: PCA-based dimension reduction, CNN-based feature extraction, and SVM-based association prediction.

TABLE 1. 5-fold cross-validation results of ELDMA on Dataset 1 and Dataset 2.

Method	Accuracy	Sensitivity	F1-score	MCC	AUC	AUPR
Dataset 1	0.9698	0.9775	0.9705	0.9403	0.9928	0.9931
Dataset 2	0.8635	0.8725	0.8623	0.8296	0.8521	0.8873

of 0.9862, 0.7426, 0.9847, and 0.9928 in global LOOCV, drug-fixed local LOOCV, miRNA-fixed local LOOCV, and 5-fold cross-validation, respectively, for Dataset 1. For Dataset 2, the model obtained AUCs of 0.8643, 0.6742, 0.8671, and 0.8521, respectively, under the above-mentioned cross-validations. The ROC curves based on Dataset 1 and Dataset 2 using 5-fold cross-validation are plotted in Figure 3. To further evaluate the model, we measured the Area under the Precision-Recall curve (AUPR) [63]. We also computed Accuracy, Sensitivity, F1-score, and Matthews correlation coefficient (MCC) as the evaluation criteria to measure the model's effectiveness, based on 5-fold cross-validation, Table 1. To decrease the variations from random sample divisions, we carried out 5-fold cross-validations ten times and averaged the results.

B. COMPARISON WITH OTHER METHODS

In order to assess the efficacy of the suggested method, we compared it with related methods predicting potential drug-miRNA associations. We compared the performance of these approaches based on Dataset 1 and Dataset 2, using the 5-fold cross-validation method. The selected methods include the network-based inference method, SMiR-NBI [19], triple-layer heterogeneous network-based approach, TLHNSMMA [21], Symmetric non-negative matrix factorization-based model, SNMFSMMA [28], and random forest-based approach, RFSMMA [22]. The first two models were network-based, the third one was matrix-based, and the latter was machine-learning-based. All these methods used the same 664 verified associations between 831 drugs and 541 miRNAs (Dataset 1) and 664 verified associations

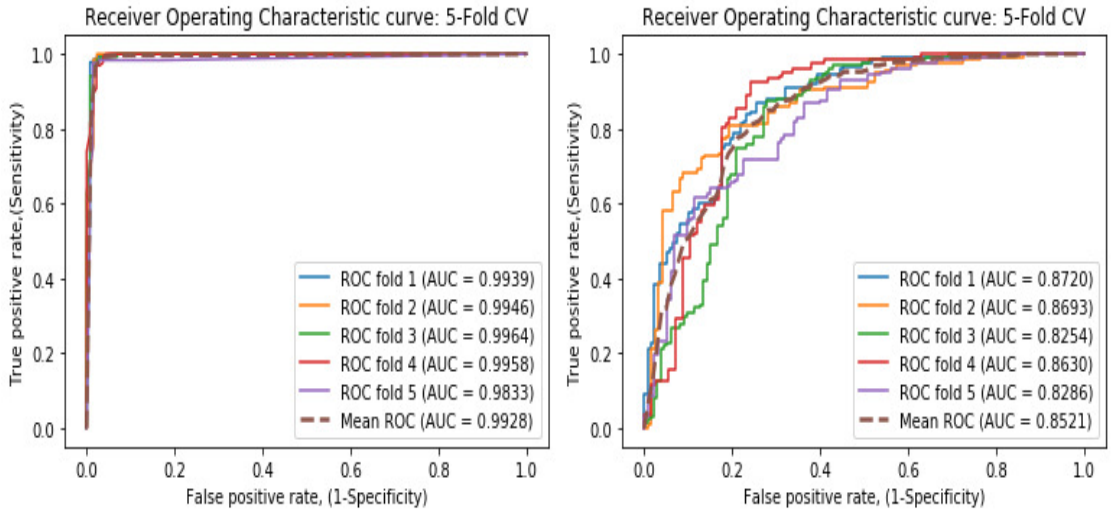

FIGURE 3. ROC curves obtained by ELDMA on Dataset 1 (Left) and Dataset 2 (Right) based on 5-fold cross-validation.

TABLE 2. Comparison of ELDMA with related methods based on Dataset1 and Dataset 2, through the AUC scores under 5-fold cross-validation.

Dataset	ELDMA*	RFSMMA	TLHNSMMA	SNMFSMMA	SMiR-NBI
Dataset 1	0.9928	0.9917	0.9851	0.9644	0.8554
Dataset 2	0.8521	0.8389	0.8168	0.8814	0.7104

TABLE 3. Comparison between ELDMA and SMiR-NBI under different cross-validations using Dataset 1 and Dataset 2.

Dataset	Method	ELDMA* (AUC)	SMiR-NBI (AUC)
Dataset 1	Global LOOCV	0.9862	0.8843
	Drug-fixed local LOOCV	0.7426	0.7497
	MiRNA-fixed local LOOCV	0.9847	0.8837
	5-fold cross-validation	0.9928	0.8554
Dataset 2	Global LOOCV	0.8643	0.7264
	Drug-fixed local LOOCV	0.6742	0.6100
	MiRNA-fixed local LOOCV	0.8671	0.7846
	5-fold cross-validation	0.8521	0.7104

between 39 drugs and 286 miRNAs (Dataset 2) for implementation. The detailed comparison results are listed in Table 2. Since there is no significant difference between the AUC scores of ELDMA, RFSMMA, SNMFSMMA, and TLHNSMMA on Dataset 1, we compared the performance of ELDMA with SMiR-NBI under different cross-validations, Table 3. The SMiR-NBI was a network-inference model predicting novel drug-miRNA associations. The comparison results, Table 2 and Table 3, reveal the robustness of the proposed approach in identifying novel drug-miRNA associations.

C. COMPARISON WITH OTHER CLASSIFIERS

We further evaluated ELDMA by comparing it to different machine learning classifiers such as deep neural networks (DNN), SVM, random forest (RF), and Decision tree. We implemented these classifiers with the proposed raw features on Dataset 1. We sent the reduced dimensional features obtained from the PCA directly to these classifiers without processing with CNN. We utilized a deep neural network with three hidden layers as it gave optimum results. We obtained AUC scores of 0.9928, 0.9904, 0.9042, 0.9379, and 0.9126 for ELDMA, RF, SVM, DNN, and Decision tree classifiers, respectively in 5-fold cross-validations. The corresponding ROC curve is shown in Figure 4. We further evaluated the model by training the DNN with the features extracted from the CNN after convolution and pooling operations, which is nothing but a CNN with multiple hidden layers. We could achieve the AUC score of 0.9808, which is about 1.2% less than that of ELDMA. With the same

TABLE 4. Top 50 drug-miRNA associations predicted by ELDMA with their evidence in the literature.

Drug	MiRNA	Evidence	Drug	MiRNA	Evidence
CID: 3385	hsa-mir-126	26062749	CID: 5757	hsa-mir-18a	24245576
CID: 3366	hsa-mir-24-1	Unconfirmed	CID: 6256	hsa-mir-126	Unconfirmed
CID: 6256	hsa-mir-24-1	Unconfirmed	CID: 60750	hsa-mir-107	Unconfirmed
CID: 60750	hsa-mir-17	23001407	CID: 3385	hsa-mir-7b	25789066
CID: 3385	hsa-mir-195	Unconfirmed	CID: 60750	hsa-mir-219a	Unconfirmed
CID: 3385	hsa-mir-221	Unconfirmed	CID: 3385	hsa-mir-146a	28466779
CID: 60750	hsa-mir-24-2	25841339	CID: 6256	hsa-mir-24-2	Unconfirmed
CID: 5790	hsa-mir-126	Unconfirmed	CID: 60750	hsa-mir-106b	Unconfirmed
CID: 3385	hsa-mir-107	Unconfirmed	CID: 3385	hsa-mir-19b-1	Unconfirmed
CID: 3366	hsa-mir-126	Unconfirmed	CID: 5757	hsa-mir-155	23568502
CID: 3385	hsa-mir-143	19843160	CID: 3366	hsa-mir-24-2	Unconfirmed
CID: 3385	hsa-mir-181a-1	Unconfirmed	CID: 3385	hsa-mir-204	27095441
CID: 5311	hsa-mir-146a	24107356	CID: 60750	hsa-mir-7e	Unconfirmed
CID: 3385	hsa-mir-145	24447928	CID: 60750	hsa-mir-125a	Unconfirmed
CID: 60750	hsa-mir-195	Unconfirmed	CID: 5757	hsa-mir-27b	26198104
CID: 3385	hsa-mir-125b-1	Unconfirmed	CID: 5578	hsa-mir-24-1	Unconfirmed
CID: 54575	hsa-mir-24-1	Unconfirmed	CID: 3366	hsa-mir-195	Unconfirmed
CID: 5790	hsa-mir-195	Unconfirmed	CID: 3385	hsa-mir-34a	25333573
CID: 3385	hsa-mir-26a-1	Unconfirmed	CID: 60750	hsa-mir-103a-1	Unconfirmed
CID: 5757	hsa-mir-27b	26198104	CID: 60750	hsa-mir-143	Unconfirmed
CID: 3385	hsa-mir-103a-1	Unconfirmed	CID: 5790	hsa-mir-195	Unconfirmed
CID: 3385	hsa-mir-29b-1	Unconfirmed	CID: 5757	hsa-mir-27a	26198104
CID: 5757	hsa-mir-221	21057537	CID: 60843	hsa-mir-24-1	Unconfirmed
CID: 6256	hsa-mir-126	Unconfirmed	CID: 3385	hsa-mir-29c	Unconfirmed
CID: 3385	hsa-mir-214	Unconfirmed	CID: 5757	hsa-mir-142	Unconfirmed

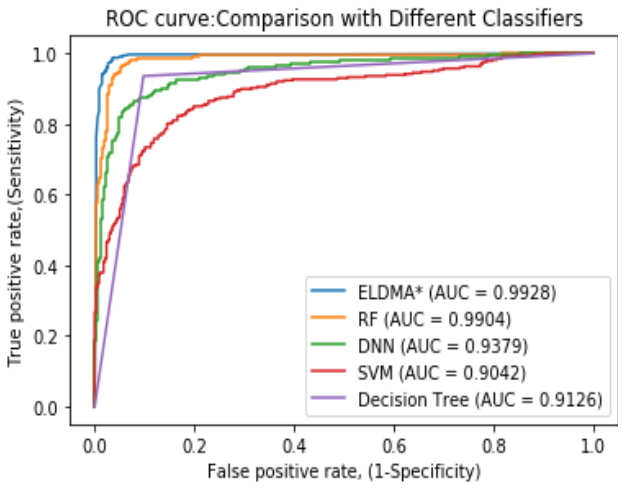

FIGURE 4. Comparison of ELDMA with different classifiers based on Dataset 1, using 5-fold cross-validation.

TABLE 5. Top predicted miRNAs associated with the drug 5-AZA-CdR, with their evidence in the literature.

Drug	MiRNA	Evidence
CID: 451668	hsa-mir-195	23333942
CID: 451668	hsa-mir-23a	Unconfirmed
CID: 451668	hsa-mir-132	26198104
CID: 451668	hsa-mir-221	Unconfirmed
CID: 451668	hsa-mir-7e	22053057
CID: 451668	hsa-mir-143	28391715
CID: 451668	hsa-mir-30a	Unconfirmed
CID: 451668	hsa-mir-7b	26708866
CID: 451668	hsa-mir-199b	24659709
CID: 451668	hsa-mir-7a-1	Unconfirmed
CID: 451668	hsa-mir-19b-1	Unconfirmed
CID: 451668	hsa-mir-143	28391715
CID: 451668	hsa-mir-15b	Unconfirmed
CID: 451668	hsa-mir-7d	26802971
CID: 451668	hsa-mir-30c-1	Unconfirmed

features, we trained the random forest classifier, but it did not show improvements on the RF. Feature extraction with CNN helped increase the AUC score of the SVM classifier by 9%, and it was the highest among other classifiers. These results indicate that ELDMA outperforms other competing classifiers in prediction power.

D. CASE STUDIES

To verify the ability of the suggested approach in inferring new drug-miRNA associations, we carried out case studies on the top-ranked results. We trained the model with all known samples and predicted association scores for all unconfirmed drug-miRNA relationships in the dataset. The predicted scores were sorted in descending order along with corresponding drug-miRNA relationships. Among the top 10, 20, and 50 predicted relationships, 3, 7, and 16 relationships were verified with the recent literature. Table 4 lists the detailed results. We further conducted a case study on the drug 5-AZA-CdR (CID:451668), an epigenetic drug that inhibits DNA methylation [64]. We evaluated our approach

by observing the top predicted miRNAs related to 5-AZA-CdR. Among the top fifteen predicted miRNAs related to 5-AZA-CdR, 8 of them have been verified with the latest literature, Table 5. The case studies indicate the reliability of the proposed method in practical applications.

IV. DISCUSSION AND CONCLUSION

MiRNAs have been demonstrated to play vital roles in the pathogenesis of multiple chronic diseases. As miRNAs have the potential to be targeted by drugs, they are being considered as novel therapeutic targets in many diseases [65]. Since drug discovery is challenging and expensive, discovering new relationships between existing drugs and miRNAs through the computational study will contribute to the miRNA-associated therapeutic strategy. Here, we presented an ensemble learning-based framework, ELDMA, that predicts potential drug-miRNA relationships. We utilized drug, miRNA similarities and experimentally confirmed drug-miRNA associations for feature construction. The constructed feature dimensions were reduced with the PCA. The resulting feature vectors were fed to CNN to extract the hidden characteristics of input data. With the extracted features, the SVM classifier was trained to predict novel drug-miRNA associations. We compared ELDMA with the previous method SMiR-NBI under different cross-validations, and the model showed significant improvements in results. Cross-validation results and case studies reveal the capability of ELDMA in drug-miRNA association predictions.

The following several factors account for the robust performance of our model. Since ensemble methods combine predictions from multiple classifiers, they are more accurate than single classifiers. Analyzing noisy samples poses great challenges to classification problems. The performance of SVM can fall when applied to noisy data [66]. The CNN-based feature extraction removes noise and retrieves the most prominent features from the input data. Training the classifier with these unique non-linear features improved the predictive performance of the model. To further enhance the model performance and reduce the high computational cost, PCA has been employed. The employment of PCA eliminated the requirement of a high-power computing unit. Besides, PCA minimized the feature dimension and thereby significantly reduced the computational complexity, both in terms of space and time. The original feature vector proposed by our approach was very long with $N_d + N_m$ size; there were $N_d \times N_m$ such features. The utilization of PCA could reduce the feature dimension by one-fourth.

The number of available training samples for this study is limited. Generally, deep architectures suffer from the problem of over-fitting when the training samples are less. Shallow learning algorithms can overcome the problems of deep learning techniques when input data size is limited. SVM works well with small datasets [67]. This study utilized the shallow machine learning algorithm SVM for classification. Although SVM is a powerful classification algorithm, it requires discriminative features. The extracted non-linear features from CNN have more discriminative power than the raw input features. So, combining the feature extraction techniques of deep architectures with shallow classifier improved the model performance. The strength of SVM lies in the kernel method. By determining a suitable kernel, SVM can be applied to resolve complex problems [68].

Numerous reliable biological datasets were incorporated in the study, such as drug side effect similarity, chemical structure similarity, gene functional consistency-based similarity for drugs and miRNAs, and disease phenotype-based similarity for miRNAs and drugs improved the predictive accuracy of ELDMA. In Network-based models, the constructed networks must be rebuilt when novel drugs or miRNAs are added to the dataset. The majority of the network-based models predicting drug-miRNA relationships have the drawback that they cannot be applied to drugs for which no known miRNAs or miRNAs for which no known drugs, associated with them in the dataset [19], [21]. The proposed method can be applied to drugs (miRNAs) with no verified miRNA (drug) relationships. Similar to other machine learning models, the suggested method can adapt to changes very well. Newly identified drugs, miRNAs, and drug-miRNA associations can be easily added to the dataset after computing similarities.

However, there are some limitations to the suggested method. Positive and negative samples are required for training ELDMA. But it is difficult or impractical to obtain the actual negative samples. So, we formed negative samples by randomly selecting unconfirmed drug-miRNA relationships. There is a chance for unverified positive samples among the selected negative samples, even though the probability is less. Besides, existing drug-miRNA associations available for this study are limited in number, and the presented model could be further improved as more verified drug-miRNA relationships are added to the dataset. Adopting more robust similarity calculation strategies can also boost the method's predictive power. Integrating more biological characteristics like miRNA sequence, expression profile similarities to the features also may produce a more robust result.

Investigating the molecular mechanism behind the therapeutic effects of drugs is essential for drug development and disease therapy. Although the problem of predicting potential drug-miRNA associations is critically important, few studies attempted to explore the target miRNAs associated with drugs systematically. The work proposed here presents a deep-learning-based computational model that identifies novel drug-miRNA relationships. The approach integrated existing drug-miRNA associations and multiple biological data sources for feature construction. CNN was used to mine the deep underlying features. With the retrieved deep features, the SVM classifier was trained to discover novel drug-miRNA associations. Cross-validation results and case studies indicate that the presented learning-based model is appropriately designed. We compared the model performance with other competing methods and different shallow and deep classifiers. We conducted experiments with both raw and

deep features, and our approach outperformed other competing classifiers. We expect the model to perform better as more and more experimentally verified drug-miRNA relationships are available. In the future, the suggested method can be used to infer novel associations between drugs and other non-coding RNAs like circular RNAs, long non-coding RNAs, etc.

Data Availability: Supplementary data associated with ELDMA are available at https://github.com/Deepthi-K523/ELDMA.

REFERENCES

[1] V. Ambros, "The functions of animal microRNAs," *Nature*, vol. 431, no. 7006, pp. 350–355, Sep. 2004.
[2] D. P. Bartel, "MicroRNAs: Genomics, biogenesis, mechanism, and function," *Cell*, vol. 116, no. 2, pp. 281–297, 2004.
[3] L.-F. Xu, Z.-P. Wu, Y. Chen, Q.-S. Zhu, S. Hamidi, and R. Navab, "MicroRNA-21 (miR-21) regulates cellular proliferation, invasion, migration, and apoptosis by targeting PTEN, RECK and Bcl-2 in lung squamous carcinoma, Gejiu city, China," *PLoS ONE*, vol. 9, no. 8, Aug. 2014, Art. no. e103698.
[4] R. C. Lee, R. L. Feinbaum, and V. Ambros, "The C. Elegans heterochronic gene lin-4 encodes small RNAs with antisense complementarity to lin-14," *Cell*, vol. 75, no. 5, pp. 843–854, Dec. 1993.
[5] M. Garofalo, G. Condorelli, and C. Croce, "MicroRNAs in diseases and drug response," *Current Opinion Pharmacol.*, vol. 8, no. 5, pp. 661–667, Oct. 2008.
[6] X. Chen, D. Xie, Q. Zhao, and Z.-H. You, "MicroRNAs and complex diseases: From experimental results to computational models," *Briefings Bioinf.*, vol. 20, no. 2, pp. 515–539, Mar. 2019.
[7] S. Volinia, M. Galasso, M. E. Sana, T. F. Wise, J. Palatini, K. Huebner, and C. M. Croce, "Breast cancer signatures for invasiveness and prognosis defined by deep sequencing of microRNA," *Proc. Nat. Acad. Sci. USA*, vol. 109, no. 8, pp. 3024–3029, Feb. 2012.
[8] J. Kim, K. Inoue, J. Ishii, W. B. Vanti, S. V. Voronov, E. Murchison, G. Hannon, and A. Abeliovich, "A MicroRNA feedback circuit in midbrain dopamine neurons," *Science*, vol. 317, no. 5842, pp. 1220–1224, 2007.
[9] S. Zhang, L. Chen, E. J. Jung, and G. A. Calin, "Targeting MicroRNAs with small molecules: From dream to reality," *Clin. Pharmacol. Therapeutics*, vol. 87, no. 6, pp. 754–758, Jun. 2010.
[10] A. Anighoro, J. Bajorath, and G. Rastelli, "Polypharmacology: Challenges and opportunities in drug discovery: Miniperspective," *J. Medicinal Chem.*, vol. 57, no. 19, pp. 7874–7887, Oct. 2014.
[11] X. Chen, N.-N. Guan, Y.-Z. Sun, J.-Q. Li, and J. Qu, "MicroRNA-small molecule association identification: From experimental results to computational models," *Briefings Bioinf.*, vol. 21, pp. 47–61, Oct. 2018.
[12] Z. Huang, J. Shi, Y. Gao, C. Cui, S. Zhang, J. Li, Y. Zhou, and Q. Cui, "HMDD V3.0: A database for experimentally supported human microRNA–disease associations," *Nucleic Acids Res.*, vol. 47, no. 1, pp. D1013–D1017, Jan. 2019.
[13] Y. Liu, X. Zeng, Z. He, and Q. Zou, "Inferring MicroRNA-disease associations by random walk on a heterogeneous network with multiple data sources," *IEEE/ACM Trans. Comput. Biol. Bioinf.*, vol. 14, no. 4, pp. 905–915, Jul. 2017.
[14] L. Fu and Q. Peng, "A deep ensemble model to predict miRNA-disease association," *Sci. Rep.*, vol. 7, no. 1, pp. 1–13, Dec. 2017.
[15] J. Li, S. Zhang, T. Liu, C. Ning, Z. Zhang, and W. Zhou, "Neural inductive matrix completion with graph convolutional networks for miRNA-disease association prediction," *Bioinformatics*, vol. 36, no. 8, pp. 2538–2546, Apr. 2020.
[16] K. Deepthi and A. S. Jereesh, "An ensemble approach for CircRNA-disease association prediction based on autoencoder and deep neural network," *Gene*, vol. 762, Dec. 2020, Art. no. 145040.
[17] G. Xie, C. Wu, G. Gu, and B. Huang, "HAUBRW: Hybrid algorithm and unbalanced bi-random walk for predicting lncRNA-disease associations," *Genomics*, vol. 112, no. 6, pp. 4777–4787, Nov. 2020.
[18] K. Deepthi and A. S. Jereesh, "Inferring potential CircRNA–disease associations via deep autoencoder-based classification," *Mol. Diagnosis Therapy*, vol. 25, pp. 87–97, Nov. 2020.
[19] J. Li, K. Lei, Z. Wu, W. Li, G. Liu, J. Liu, F. Cheng, and Y. Tang, "Network-based identification of microRNAs as potential pharmacogenomic biomarkers for anticancer drugs," *Oncotarget*, vol. 7, no. 29, pp. 45584–45596, Jul. 2016.
[20] Y. Lv, S. Wang, F. Meng, L. Yang, Z. Wang, J. Wang, X. Chen, W. Jiang, Y. Li, and X. Li, "Identifying novel associations between small molecules and miRNAs based on integrated molecular networks," *Bioinformatics*, vol. 31, no. 22, pp. 3638–3644, 2015.
[21] J. Qu, X. Chen, Y.-Z. Sun, J.-Q. Li, and Z. Ming, "Inferring potential small molecule–miRNA association based on triple layer heterogeneous network," *J. Cheminformatics*, vol. 10, no. 1, pp. 1–14, Dec. 2018.
[22] C. C. Wang, X. Chen, J. Qu, Y. Z. Sun, and J. Q. Li, "RFSMMA: A new computational model to identify and prioritize potential small molecule–miRNA associations," *J. Chem. Inf. Model.*, vol. 59, no. 4, pp. 1668–1679, 2019.
[23] J. Qu, X. Chen, Y.-Z. Sun, Y. Zhao, S.-B. Cai, Z. Ming, Z.-H. You, and J.-Q. Li, "In silico prediction of small molecule-miRNA associations based on the HeteSim algorithm," *Mol. Therapy-Nucleic Acids*, vol. 14, pp. 274–286, Mar. 2019.
[24] C. Shi, X. Kong, Y. Huang, P. S. Yu, and B. Wu, "HeteSim: A general framework for relevance measure in heterogeneous networks," *IEEE Trans. Knowl. Data Eng.*, vol. 26, no. 10, pp. 2479–2492, Oct. 2014.
[25] N.-N. Guan, Y.-Z. Sun, Z. Ming, J.-Q. Li, and X. Chen, "Prediction of potential small molecule-associated MicroRNAs using graphlet interaction," *Frontiers Pharmacol.*, vol. 9, p. 1152, Oct. 2018.
[26] K. Deepthi and A. S. Jereesh, "Drug repositioning based on the target microRNAs using bilateral-inductive matrix completion," *Mol. Genet. Genomics*, vol. 295, no. 5, pp. 1305–1314, Sep. 2020.
[27] F. Liu, L. Peng, G. Tian, J. Yang, H. Chen, Q. Hu, X. Liu, and L. Zhou, "Identifying small molecule-miRNA associations based on credible negative sample selection and random walk," *Frontiers Bioeng. Biotechnol.*, vol. 8, p. 131, Mar. 2020.
[28] Y. Zhao, X. Chen, J. Yin, and J. Qu, "SNMFSMMA: Using symmetric nonnegative matrix factorization and kronecker regularized least squares to predict potential small molecule-microRNA association," *RNA Biol.*, vol. 17, no. 2, pp. 281–291, Feb. 2020.
[29] C. C. Wang and X. Chen, "A unified framework for the prediction of small molecule-microRNA association based on cross-layer dependency inference on multilayered networks," *J. Chem. Inf. Model.*, vol. 59, no. 12, pp. 5281–5293, 2019.
[30] C. Shen, J. Luo, W. Ouyang, P. Ding, and H. Wu, "Identification of small molecule–miRNA associations with graph regularization techniques in heterogeneous networks," *J. Chem. Inf. Model.*, vol. 60, no. 12, pp. 6709–6721, 2020.
[31] J. Yin, X. Chen, C. C. Wang, Y. Zhao, and Y. Z. Sun, "Prediction of small molecule–microRNA associations by sparse learning and heterogeneous graph inference," *Mol. Pharmaceutics*, vol. 16, no. 7, pp. 3157–3166, 2019.
[32] J. Luo, C. Shen, Z. Lai, J. Cai, and P. Ding, "Incorporating clinical, chemical and biological information for predicting small molecule-microRNA associations based on non-negative matrix factorization," *IEEE/ACM Trans. Comput. Biol. Bioinf.*, early access, Feb. 24, 2020, doi: 10.1109/TCBB.2020.2975780.
[33] X. Liu, S. Wang, F. Meng, J. Wang, Y. Zhang, E. Dai, X. Yu, X. Li, and W. Jiang, "SM2miR: A database of the experimentally validated small molecules' effects on microRNA expression," *Bioinformatics*, vol. 29, no. 3, pp. 409–411, Feb. 2013.
[34] C. Knox, V. Law, T. Jewison, P. Liu, S. Ly, A. Frolkis, A. Pon, K. Banco, C. Mak, V. Neveu, Y. Djoumbou, R. Eisner, A. C. Guo, and D. S. Wishart, "DrugBank 3.0: A comprehensive resource for 'omics' research on drugs," *Nucleic Acids Res.*, vol. 39, pp. D1035–D1041, Jan. 2011.
[35] Y. Wang, J. Xiao, T. O. Suzek, J. Zhang, J. Wang, and S. H. Bryant, "PubChem: A public information system for analyzing bioactivities of small molecules," *Nucleic Acids Res.*, vol. 37, pp. W623–W633, Jul. 2009.
[36] Z. Huang, J. Shi, Y. Gao, C. Cui, S. Zhang, J. Li, Y. Zhou, and Q. Cui, "HMDD v3.0: A database for experimentally supported human microRNA–disease associations," *Nucleic Acids Res.*, vol. 47, no. 1, pp. D1070–D1074, Jan. 2019.
[37] A. Ruepp, A. Kowarsch, D. Schmidl, F. Buggenthin, B. Brauner, I. Dunger, and F. J. Theis, "PhenomiR: A knowledgebase for microRNA expression in diseases and biological processes," *Genome Biol.*, vol. 11, no. 1, pp. 1–11, 2010.

[38] Q. Jiang, Y. Wang, Y. Hao, L. Juan, M. Teng, X. Zhang, M. Li, G. Wang, and Y. Liu, "MiR2Disease: A manually curated database for microRNA deregulation in human disease," *Nucleic Acids Res.*, vol. 37, pp. D98–D104, Jan. 2009.
[39] M. Kanehisa, S. Goto, Y. Sato, M. Furumichi, and M. Tanabe, "KEGG for integration and interpretation of large-scale molecular data sets," *Nucleic Acids Res.*, vol. 40, no. 1, pp. D109–D114, Jan. 2012.
[40] A. Gottlieb, G. Y. Stein, E. Ruppin, and R. Sharan, "PREDICT: A method for inferring novel drug indications with application to personalized medicine," *Mol. Syst. Biol.*, vol. 7, no. 1, p. 496, Jan. 2011.
[41] M. Kuhn, I. Letunic, L. J. Jensen, and P. Bork, "The SIDER database of drugs and side effects," *Nucleic Acids Res.*, vol. 44, no. 1, pp. D1075–D1079, Jan. 2016.
[42] R. C. Friedman, K. K.-H. Farh, C. B. Burge, and D. P. Bartel, "Most mammalian mRNAs are conserved targets of microRNAs," *Genome Res.*, vol. 19, no. 1, pp. 92–105, Oct. 2008.
[43] S. Lv, Y. Li, Q. Wang, S. Ning, T. Huang, P. Wang, J. Sun, Y. Zheng, W. Liu, J. Ai, and X. Li, "A novel method to quantify gene set functional association based on gene ontology," *J. Roy. Soc. Interface*, vol. 9, no. 70, pp. 1063–1072, May 2012.
[44] F. Zhu, Z. Shi, C. Qin, L. Tao, X. Liu, F. Xu, L. Zhang, Y. Song, X. Liu, J. Zhang, and Y. Chen, "Therapeutic target database update 2012: A resource for facilitating target-oriented drug discovery," *Nucleic Acids Res.*, vol. 40, no. 1, pp. D1128–D1136, 2012.
[45] A. P. Davis, C. G. Murphy, M. C. Rosenstein, R. Johnson, J. M. Lay, D. Sciaky, K. Lennon-Hopkins, B. L. King, C. Saraceni-Richards, T. C. Wiegers, and C. J. Mattingly, "The comparative toxicogenomics database: Update 2013," *Nucleic Acids Res.*, vol. 41, no. 1, pp. D1104–D1114, 2013.
[46] M. Hattori, Y. Okuno, S. Goto, and M. Kanehisa, "Development of a chemical structure comparison method for integrated analysis of chemical and genomic information in the metabolic pathways," *J. Amer. Chem. Soc.*, vol. 125, no. 39, pp. 11853–11865, Oct. 2003.
[47] Y. LeCun, B. Boser, J. S. Denker, D. Henderson, R. E. Howard, W. Hubbard, and L. D. Jackel, "Backpropagation applied to handwritten zip code recognition," *Neural Comput.*, vol. 1, no. 4, pp. 541–551, Dec. 1989.
[48] H.-J. Jiang, Z.-H. You, and Y.-A. Huang, "Predicting drug–disease associations via sigmoid kernel-based convolutional neural networks," *J. Transl. Med.*, vol. 17, no. 1, pp. 1–11, Dec. 2019.
[49] C. Fan, X. Lei, and Y. Pan, "Prioritizing CircRNA–disease associations with convolutional neural network based on multiple similarity feature fusion," *Frontiers Genet.*, vol. 11, p. 1042, Sep. 2020.
[50] P. Xuan, Y. Cao, T. Zhang, R. Kong, and Z. Zhang, "Dual convolutional neural networks with attention mechanisms based method for predicting disease-related lncRNA genes," *Frontiers Genet.*, vol. 10, p. 416, May 2019.
[51] C. Cortes and V. Vapnik, "Support-vector networks," *Mach. Learn.*, vol. 20, no. 3, pp. 273–297, 1995.
[52] T. B. Trafalis and R. C. Gilbert, "Robust classification and regression using support vector machines," *Eur. J. Oper. Res.*, vol. 173, no. 3, pp. 893–909, 2006.
[53] X. Chen, Q.-F. Wu, and G.-Y. Yan, "RKNNMDA: Ranking-based KNN for miRNA-disease association prediction," *RNA Biol.*, vol. 14, no. 7, pp. 952–962, Jul. 2017.
[54] W. Lan, M. Li, K. Zhao, J. Liu, F. X. Wu, Y. Pan, and J. Wang, "LDAP: A Web server for lncRNA-disease association prediction," *Bioinformatics*, vol. 33, no. 3, pp. 458–460, 2017.
[55] C. Pian, S. Mao, G. Zhang, J. Du, F. Li, S. Y. Leung, and X. Fan, "Discovering cancer-related miRNAs from miRNA-target interactions by support vector machines," *Mol. Therapy-Nucleic Acids*, vol. 19, pp. 1423–1433, Mar. 2020.
[56] K. Sachdev and M. K. Gupta, "An improved approach for predicting drug target interactions," in *Proc. Int. Conf. Issues Challenges Intell. Comput. Techn. (ICICT)*, vol. 1, Sep. 2019, pp. 1–5.
[57] J. Lin, H. Chen, S. Li, Y. Liu, X. Li, and B. Yu, "Accurate prediction of potential druggable proteins based on genetic algorithm and bagging-SVM ensemble classifier," *Artif. Intell. Med.*, vol. 98, pp. 35–47, Jul. 2019.
[58] P.-W. Hu, K. C. C. Chan, and Z.-H. You, "Large-scale prediction of drug-target interactions from deep representations," in *Proc. Int. Joint Conf. Neural Netw. (IJCNN)*, Jul. 2016, pp. 1236–1243.
[59] X. Chen, Y. Gong, D.-H. Zhang, Z.-H. You, and Z.-W. Li, "DRMDA: Deep representations-based miRNA-disease association prediction," *J. Cellular Mol. Med.*, vol. 22, no. 1, pp. 472–485, Jan. 2018.
[60] J. N. Mandrekar, "Receiver operating characteristic curve in diagnostic test assessment," *J. Thoracic Oncol.*, vol. 5, no. 9, pp. 1315–1316, Sep. 2010.
[61] R. Kumar and A. Indrayan, "Receiver operating characteristic (ROC) curve for medical researchers," *Indian Pediatrics*, vol. 48, no. 4, pp. 277–287, 2011.
[62] A. P. Bradley, "The use of the area under the ROC curve in the evaluation of machine learning algorithms," *Pattern Recognit.*, vol. 30, no. 7, pp. 1145–1159, Jul. 1997.
[63] K. Boyd, K. H. Eng, and C. D. Page, "Area under the precision-recall curve: Point estimates and confidence intervals," in *Proc. Joint Eur. Conf. Mach. Learn. Knowl. Discovery Databases*. Berlin, Germany: Springer, Sep. 2013, pp. 451–466.
[64] M. Karahoca and R. L. Momparler, "Pharmacokinetic and pharmacodynamic analysis of 5-aza-2'-deoxycytidine (decitabine) in the design of its dose-schedule for cancer therapy," *Clin. Epigenetics*, vol. 5, no. 1, pp. 1–16, Dec. 2013.
[65] R. Garzon, G. Marcucci, and C. M. Croce, "Targeting microRNAs in cancer: Rationale, strategies and challenges," *Nature Rev. Drug Discovery*, vol. 9, no. 10, pp. 775–789, Oct. 2010.
[66] S. Anwar and R. Ismal, "Robustness analysis of artificial neural networks and support vector machine in making prediction," in *Proc. IEEE 9th Int. Symp. Parallel Distrib. Process. Appl.*, May 2011, pp. 256–261.
[67] K. Pasupa and W. Sunhem, "A comparison between shallow and deep architecture classifiers on small dataset," in *Proc. 8th Int. Conf. Inf. Technol. Electr. Eng. (ICITEE)*, Oct. 2016, pp. 1–6.
[68] Z. Liu, M. J. Zuo, X. Zhao, and H. Xu, "An analytical approach to fast parameter selection of Gaussian RBF kernel for support vector machine," *J. Inf. Sci. Eng.*, vol. 31, no. 2, pp. 691–710, 2015.

K. DEEPTHI (Member, IEEE) received the master's degree in computer science and engineering from the VMKV Engineering College, India, in 2008. She is currently pursuing the Ph.D. degree with the Cochin University of Science and Technology, Kochi, India. She is also an Assistant Professor with the Department of Computer Science, College of Engineering Vadakara (CAPE, Government of Kerala), Kozhikode, India. Her research interests include computational biology, algorithms for bioinformatics, and machine learning.

A. S. JEREESH received the bachelor's degree in computer science and engineering from the Rajiv Gandhi Institute of Technology, Kottayam, in 2007, the master's degree in computer science and engineering (information security) from the National Institute of Technology Calicut, in 2010, and the Ph.D. degree from the Department of Computer Science and Engineering, National Institute of Technology Calicut, in 2015. He started his carrier as an Assistant Professor at the Department of Computer Science, Adi Shankara Institute of Science and Technology, Kalady, in 2014. Later, he joined the Department of Computer Science, CUSAT, in October 2015. He is currently an Assistant Professor with the Department of Computer Science, Cochin University of Science and Technology. His research interests include the image processing, bioinformatics, data mining, and evolutionary algorithms.